Resolution of Conformational States of Spin-Labeled Myosin during Steady-State ATP Hydrolysis†

Vincent A. Barnett and David D. Thomas*
Department of Biochemistry, University of Minnesota Medical School, The University of Minnesota, Minneapolis, Minnesota 55455

Received May 21, 1986; Revised Manuscript Received September 16, 1986

ABSTRACT: We have measured the conventional electron paramagnetic resonance (EPR) spectrum of spin-labeled myosin filaments as a function of the nucleotide occupancy of the active site of the enzyme. The probe used was 4-(2-iodoacetamido)-2,2,6,6-tetramethylpiperidine-1-oxyl (IASL), which reacts specifically with sulfhydryl 1 of the myosin head. In the absence of nucleotide, the probe remains strongly immobilized (rigidly attached to the myosin head) so that no nanosecond rotational motions are detectable. When MgADP is added to IASL-labeled myosin filaments (T = 20 °C), the probe mobility increases slightly. During steady-state MgADP hydrolysis (T = 20 °C), the probe undergoes large-amplitude nanosecond rotational motion. These results are consistent with previous studies of myosin monomers, heavy meromyosin, and myosin subfragment 1. Isoclinic points observed in overlays of sequential EPR spectra recorded during ATP hydrolysis strongly suggest that the probes fall into *two motional classes*, separated by approximately an order of magnitude in effective rotational correlation time. Both of the observed states are distinct from the conformation of myosin in the absence of nucleotides, and the spectrum of the less mobile population is indistinguishable from that observed in the presence of MgADP. The addition of ADP and vanadate to IASL-myosin gives rise to two motional classes virtually identical with those observed in the presence of ATP, but the relative concentrations of the spin populations are significantly different. We have quantitated the percentage of myosin in each motional state during ATP hydrolysis. The result agrees well with the predicted percentages in the two predominant chemical states in the myosin ATPase cycle. Spectra obtained in the presence of nucleotide analogues permit us to assign the conformational states to specific chemical states. We propose that the two motional classes represent two distinct local conformations of myosin that are in exchange with one another during the ATP hydrolysis reaction cycle.

In muscle, the transduction of chemical energy into mechanical work is primarily mediated by the interactions of the proteins actin and myosin. These proteins form independent, interdigitating filaments (thin = actin filaments and thick = myosin filaments) that slide past one another as a muscle shortens. Because of the ultrastructural arrangement of myosin monomers in thick filaments, and the residence of adenosine 5′-triphosphate (ATP)[1]-hydrolysis and actin-binding sites on each of its globular "heads", proposals that involve local and global conformational changes of this protein have played fundamental roles in the development of models for the molecular mechanism of muscle contraction [Huxley, 1969; Huxley & Simmons, 1971; Bagshaw & Trentham, 1974; reviewed by Highsmith & Cooke (1983), Cooke (1986), and Thomas (1987)].

Myosin undergoes local conformational changes during steady-state ATP hydrolysis that can be detected by changes in UV absorbance (Morita, 1967) and intrinsic fluorescence (Werber et al., 1972). The changes in intrinsic fluorescence have received considerable attention and have been associated with chemical intermediates of the ATP hydrolysis reaction depicted in Scheme I (Bagshaw & Trentham, 1974; Trentham et al., 1976), where each asterisk represents a change in intrinsic fluorescence intensity. Kinetic measurements indicate that the predominant myosin–nucleotide species during steady-state ATP hydrolysis by myosin (at 20 °C, under physiological ionic conditions) are the M*ATP and M**ADP·P_i states (in a ratio of approximately 1:9) and that the interconversion between the two states is rapid (k_+ = 160 s^{-1}, k_- = 18 s^{-1}; Geeves & Trentham, 1982).

Scheme I

$$M \leftrightarrow M^*ATP \leftrightarrow M^{**}ADP{\cdot}P_i \leftrightarrow M^*ADP{\cdot}P_i \leftrightarrow M^*ADP \leftrightarrow M$$

Several other spectroscopic techniques have been used to look for nucleotide-induced changes in myosin structure [for a review, see Morales et al. (1982)]. ATP and ATP analogues have no measurable effect on the ^1H NMR spectrum of S-1 (Highsmith et al., 1979), suggesting a lack of a substantial global conformational change. However, ADP (or AMPPNP) induces a change in the chemical shift of a ^{19}F NMR probe attached to sulfhydryl 1 (SH_1) on S-1 (Shriver & Sykes, 1982).

† This work was supported by grants from the National Institutes of Health (GM27906 and AM32961), the American Heart Association, the National Science Foundation (PCM 8004612), and the Muscular Dystrophy Association of America. D.D.T. was supported by a Research Career Development award from the National Institutes of Health and is currently supported by an Established Investigatorship from the American Heart Association. V.A.B. was partially supported by a predoctoral fellowship from the National Science Foundation.

[1] Abbreviations: ADP, adenosine 5′-diphosphate; AMPPNP, 5′-adenylyl imidodiphosphate; ATP, adenosine 5′-triphosphate; ATPγS, adenosine 5′-*O*-(3-thiotriphosphate); Ap_5A, P^1,P^5-di(adenosine-5′) pentaphosphate; EPPS, *N*-(2-hydroxyethyl)piperazine-*N*′-3-propanesulfonic acid; IASL, 4-(2-iodoacetamido)-2,2,6,6-tetramethylpiperidine-1-oxyl; MOPS, 3-(*N*-morpholino)propanesulfonic acid; MSL, 4-maleimido-2,2,6,6-tetramethylpiperidine-1-oxyl; PAR, 4-(2-pyridylazo)resorcinol; V_i, orthovanadate; EPR, electron paramagnetic resonance; S-1, myosin subfragment 1; DMF, dimethylformamide; EDTA, ethylenediaminetetraacetic acid; DTT, dithiothreitol; EGTA, ethylene glycol bis(β-aminoethyl ether)-*N*,*N*,*N*′,*N*′-tetraacetic acid; IAA, iodoacetic acid; CP, creatine phosphate; CPK, creatine phosphokinase.

0006-2960/87/0426-0314$01.50/0

In previous studies of spin-labeled myosin, it was determined that nitroxide spin-labels conjugated with an iodoacetamide group (IASL) selectively alkylate SH_1 of myosin and are sensitive to the binding of nucleotides to myosin's active site (Seidel et al., 1970; Seidel & Gergely, 1971, 1973; Stone, 1970; Bagshaw & Reed, 1976; Furukawa & Tonomura, 1982). In the absence of nucleotides, the probe is rigidly attached to the myosin molecule, and the motion of the probe reflects the overall rotational mobility of the myosin head (Thomas et al., 1975). However, ADP mobilizes the probe slightly, and ATP mobilizes it much more (Seidel & Gergely, 1973). The ADP-induced line shape was originally interpreted as corresponding to the M* state of myosin and the ATP-induced line shape as the M** state (Seidel & Gergely, 1973).

The myosin ATPase is inhibited by orthovanadate [VO_4^{3-} (V_i)], a phosphate analogue, due to the formation of a myosin–ADP–vanadate complex whose half-life is on the order of 3 days (Goodno, 1979). Wells and Bagshaw (1984) have reported that, while spin-labeling reduces the stability of the myosin–ADP–vanadate complex, the addition of ADP and orthovanadate (V_i) to IASL-labeled myosin causes changes in the conventional EPR spectrum that are long-lived on the time scale of an EPR experiment (minutes). The EPR spectrum they obtained in the presence of ADP and vanadate shows that the probe becomes quite mobile. Since this probe mobilization is similar to that induced by the addition of ATP alone, they suggested that the myosin–ADP–vanadate complex (M^{*}·ADP·V_i) is a good analogue of the predominant conformational state during steady-state ATP hydrolysis (M**ADP·P_i). However, the signal-to-noise ratio for these experiments was too low to allow quantitative comparison.

Most of the previous studies of myosin's conformational state have used myosin monomers (high ionic strength, [KCl] $\geq$ 0.35 M) or proteolytic fragments of myosin. In the present study, we focus on myosin under more physiological ionic conditions where it forms thick filaments similar to those in muscle. In several previous studies on spin-labeled myosin, the labeled myosin had more than one population of sulfhydryls modified, preventing quantitative analysis of spectral changes. The quantitative analysis of EPR spectra in terms of multiple components requires (a) specific labeling, (b) computer analysis to deconvolute the individual components, and (c) a signal to noise ratio which is high enough to clearly distinguish minor components.

In the present study, we reinvestigate the nucleotide-dependent changes in the conventional EPR spectrum of IASL-labeled myosin filaments with the goal of deconvoluting the complex line shape that occurs in the presence of ATP and determining quantitatively the relative concentrations of conformational intermediates during ATP hydrolysis. We have developed spin-labeling procedures to achieve rigorously specific labeling, so that all detectable probes are attached to SH_1, permitting us to analyze spectra in terms of multiple conformational states of identical molecules. In addition, we have used computer analysis of digitized spectra to provide (a) rigorous tests of the hypothesis of multiple states and (b) quantitative measurement of the fractions of molecules in these states.

Materials and Methods

Reagents and Buffers. ATP, ADP, AMPPNP, PAR, MOPS, and EPPS were purchased from Sigma Chemical Co. (St. Louis, MO). ATPγS and Ap_5A were obtained from Boehringer Mannheim Biochemicals (Indianapolis, IN). Glycerol (Spectranalyzed, ≥99.9% pure), for use in the storage buffer for spin-labeled myosin, and Na_3VO_4 were purchased from Fisher Scientific (Pittsburgh, PA). The spin-labels IASL and MSL were obtained from Aldrich Chemical Co. (Milwaukee, WI). All other chemicals were of reagent grade and of the highest quality available. All buffers were prepared as described in Table I unless specifically described in the text.

Preparation and Characterization of Vanadate Solutions. A stock solution of 200 mM Na_3VO_4 was prepared as described by Goodno (1979). The concentration of the Na_3VO_4 stock solution at pH 10.0 was determined by using the absorbance of vanadate at 260 nm (ϵ_{260} = 3430 M^{-1} cm^{-1}; Reiger, 1973). All subsequent solutions were made by dilutions of the stock solution into buffers at pH 8.0. The vanadate concentration in the presence of myosin was determined by using the procedure of Pribil (1972) as modified by Goodno (1979). To a 1.0-mL sample in LB was added 100 μL of 1.0 M imidazole (pH 6.0), followed by the addition of 100 μL of 4-(2-pyridylazo)resorcinol (PAR). After 30 min of color development, the absorbance was read at 550 nm and compared to a standard curve. Vanadate solutions are known to self-polymerize in a pH- and concentration-dependent manner (Reiger, 1973; Chasten, 1983). While the polymer decavanadate has no significant contribution at pH 8.0, trimers of vanadate form readily (Chaster, 1983; Wells & Bagshaw, 1984). The apparent equilibrium constant at pH 8.0 for the reaction $3H_2VO_4^- \leftrightarrow V_3O_9 + 3H_2O$ (K_p') is 1×10^{-5} M^2 (Wells & Bagshaw, 1984). Given this value for K_p', any vanadate in excess of 3.2 mM is likely to be in the form of the trimer (Wells & Bagshaw, 1984).

Preparation of Spin-Labeled Myosin. Myosin was isolated and purified from myofibrils of the white back and leg muscles of New Zealand white rabbits as described by Eads et al. (1984) and stored at −20 °C in MSB for up to 6 months. Spin-labeling of myosin with IASL or MSL was accomplished by using a slight modifications of the procedures of Thomas et al. (1980), as follows. To prepare IASL-myosin, the spin-label (in a 100 mM stock solution in DMF, stored under liquid nitrogen) was diluted to a concentration of 1.0 mM in LB immediately before labeling. A small amount of this diluted stock solution was saved for later use as a concentration standard (see below). This spin-label solution was added to a myosin filament suspension (10 mg/mL, 20.8 μM myosin and 41.6 μM SH_1) in LB (pH 7.0) to a concentration of 27 μM, corresponding to 0.65 probe per SH_1. After 12-h incubation at 0 °C, the spin-label concentration was raised to a final concentration of 53 μM (1.3 probes per SH_1), and the reaction was allowed to continue an additional 4 h. For labeling myosin with MSL, a myosin filament suspension was prepared at 10 mg/mL in LB (pH 6.5). MSL (in a 100 mM stock solution in DMF, stored under liquid nitrogen) was diluted as described above for IASL and then added to a final concentration of 80 μM (1.9 probes per SH_1), and the mixture was incubated at 0 °C for 20 min with occasional stirring. After incubation with either IASL or MSL, the spin-labeled myosin was diluted by a factor of 2 with the appropriate LB and centrifuged at 3000*g* for 10 min. The pellet was then resuspended with LB and centrifuged at 12000*g* for 10 min. The pellet of the second centrifugation was dissolved by the gradual addition of $^1/_4$th volume of 2.5 M KCl, followed by the addition of $^1/_{10}$th volume of 100 mM $K_3Fe(CN)_6$ to destroy the signal from labels not on SH_1 (Thomas et al., 1980; Graceffa & Seidel, 1980). IASL-labeled samples were dialyzed vs. MB at 4 °C until all ferricyanide was removed, as evidenced by the absence of its yellow color. MSL samples were incubated in ferricyanide for 30 min prior to the initiation of dialysis. After dialysis to remove ferricyanide, spin-labeled

Table I: Chemical Constituents of Buffers[a]

buffer	[nucleotide] (mM)	[V_i] (mM)	[CP] (mM)	[CPK] (IU/mL)	[Ap_5A] (mM)	[$MgCl_2$] (mM)	[KCl] (mM)	[KOAc] (mM)	[EDTA] (mM)	[EGTA] (mM)	[MOPS] (mM), pH 7.0	[EPPS] (mM), pH 8.0	[NaN_3] (mM)	[DTT] (mM)	[glycerol] (% v/v)
LB							50.0		0.10		10.0		1.0		
MB							500.0		0.10		5.0				
MSB							500.0		0.50		20.0			0.50	50
no Nuc[b]	0.0					6.0		135.0		1.0		20.0			
ATP	5.0		20.0	233		6.0		60.0		1.0		20.0			
ATP + V_i	5.0	5.0	20.0	233		6.0				1.0		20.0			
ADP	5.0				0.03	6.0		124.0		1.0		20.0			
ADP + V_i	5.0	5.0			0.03	6.0		64.0		1.0		20.0			
AMPPNP	5.0					6.0		120.0		1.0		20.0			
ATPγS	5.0					6.0		60.0		1.0		20.0			

[a] Components of buffers. The pH of each buffer was measured at 25 °C. Labeling of myosin with MSL was done at pH 6.5. [b] No nucleotide.

myosin was either used immediately or dialyzed vs. MSB minus dithiothreitol at 4 °C for 18 h and stored at −20 °C until needed.

EPR Sample Preparation. Glycerol was removed from myosin samples in storage buffer by overnight dialysis into MB. This was followed by dialysis into a filament-forming buffer at pH 8.0 (LB with EPPS in place of MOPS, pH 8.0). The filaments were washed into the appropriate nucleotide-containing buffers (minus the nucleotides or vanadate) by repeated centrifugations and resuspensions. Nucleotides and/or vanadate was added immediately prior to EPR data acquisition to a concentration of 5 mM. The concentration of potassium acetate was varied to maintain an ionic strength of 0.15 M.

Protein Concentration. The protein concentrations of myosin suspensions were determined by using UV absorbance scans. Calculation of the concentration of myosin samples was accomplished by using the absorbance of myosin at 280 nm [A_{280}(1 mg/mL) = 0.54; Gellert & Englander, 1963] in the following formula: $(A_{280} - A_{320})/0.54$ = [myosin], where the absorbance at 320 nm represents the contribution of scattered light to the myosin absorbance. Molar concentrations of myosin solutions were calculated by using 480 000 (Tonomura et al., 1966) for the molecular weight of myosin.

ATPase Activity. Myosin ATPase activities were measured essentially as described by Eads et al. (1984) by determining the rate of release of inorganic phosphate (P_i). The K^+/EDTA–ATPase activity was assayed at 25 °C in a solution containing 5 mM EDTA, 0.60 M KCl, and 50 mM MOPS (pH 7.5), while the buffer for Ca^{2+}/K^+-ATPase activities contained 10 mM $CaCl_2$, 0.60 M KCl, and 50 mM MOPS (pH 7.5).

EPR Spectroscopy. Conventional (V_1) EPR experiments were performed as described previously (Barnett & Thomas, 1984; Thomas et al., 1980; Thomas & Cooke, 1980), using either a Varian E-109 spectrometer (Varian Associates, Palo Alto, CA) or a Bruker ER200D-SRC spectrometer (IBM Instruments, Danbury, CT). Saturation-transfer EPR (ST-EPR) spectra were acquired as described by Squier and Thomas (1986). Spectra were digitized and analyzed by means of a North Star computer interfaced to the Varian spectrometer (Lipscomb & Salo, 1983) or either a Nicolet 1180E or a Zenith-150 computer interfaced to the Bruker spectrometer. Spectra were recorded over a temperature range of 0–40 °C. The temperature for all spectra shown in the figures was 20 °C.

Spin Quantitation. The molar concentration of spins was determined by double integration of the digitized conventional (V_1) EPR spectra, calibrated with a 0.5 mM standard spin-label solution prepared from the same stock solution used for labeling.

Specificity of Labeling. The modification of SH_1 is known to cause characteristic changes in myosin ATPase activity (Sekine & Kielley, 1964; Crowder & Cooke, 1984). In particular, the fractional inhibition of the K^+/EDTA–ATPase has been demonstrated to be a sensitive indicator of the fraction of SH_1 groups modified, declining linearly as the percentage of SH_1 groups modified increases. Assays on IASL-myosin suspensions used in this study typically exhibited about an 80% inhibition of K^+/EDTA–ATPase activity, indicating that the fraction of SH_1 groups labeled was 0.80. For MSL-labeled myosin, the fraction of SH_1 groups modified was typically about 0.70. Quantitation of the spin concentration showed that the number of spin-labels bound per myosin head never exceeded the fraction of SH_1 groups blocked by more than

Scheme II

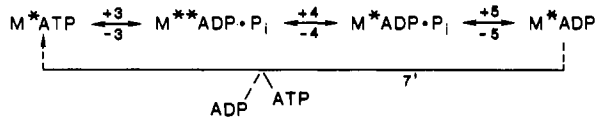

10%, indicating that at least 90% of the spin-labels are attached to SH_1. The ferricyanide treatment removed only aboout 5–10% of the IASL signal and about 30% of the MSL signal; the decrease was mainly in the signal component due to weakly immobilized spins (Thomas et al., 1980). Competition experiments indicated that the spins remaining after ferricyanide treatment are attached to the same site for both spin-labels.

EPR Spectral Parameters. Nanosecond rotational motions were analyzed by measuring the conventional (V_1) EPR spectral parameters. $2T_\parallel'$, the separation in gauss between the outermost extrema, and Δ_L, the width in gauss at half-height of the low-field peak (Mason & Freed, 1974), were measured as illustrated in Figure 1. An increase in either the rate or the amplitude of submicrosecond motion (corresponding to a decrease in the rotational correlation time, τ_r, or order parameter, S, respectively) results in a decrease in $2T_\parallel'$ and an increase in Δ_L. $2T_\parallel'$ usually provides better precision but is more sensitive to changes in local polarity. The use of both parameters reduces the ambiguity as to the cause of the spectral changes.

Spectral Subtractions. Digitized spectra were normalized to the same number of spins (by dividing by the double integral of the V_1 spectrum) before computer subtraction of one spectrum from another. The end point, i.e., the fraction of spectrum B required to convert a multicomponent spectrum A into a single-component spectrum C, was determined as follows: A feature much more prominent in spectrum B than in spectrum A was selected, and the fraction of spectrum B subtracted was increased until this feature was removed from spectrum A without inversion of phase. Alternatively, two end-point spectra (B and C) were chosen and then added in linear combination to produce a composite spectrum A'. The best fit to spectrum A was obtained by varying the relative fractions of spectra B and C until the residual obtained by subtraction of A' from A was a minimum. Comparison of composite spectra with the spectrum of myosin + ATP was done on a Zenith-150 computer using a program developed by Piotr Fajer and Robert L. H. Bennett.

Computer Simulation of ATPase Kinetics. A computer program was developed to simulate the myosin ATPase reaction under conditions where ATP is assumed to be saturating (see Scheme II). The program written in FORTRAN and run on a Zenith-150 computer was developed from a fouth-order Runge–Kutta integration algorithm for a system of differential equations written by K. B. Wigard (Wigard, 1974). The simulations were used to determine the relationship (if any) of the ratios of the predominant motional states observed to concentrations of intermediates in the myosin ATPase cycle. The equations used in the simulation algorithm were as follows:

$$d(M^*ATP)/dt = k_{-3}(M^{**}ADP{\cdot}P) - k_3(M^*ATP) \quad (1)$$

$$d(M^{**}ADP{\cdot}P)/dt = k_{-4}(M^*ADP{\cdot}P) + k_3(M^*ATP) - k_{-3}(M^*ADP{\cdot}P) - k_4(M^{**}ADP{\cdot}P) \quad (2)$$

$$d(M^*ADP{\cdot}P)/dt = k_{-5}(M^*ADP) + k_4(M^{**}ADP{\cdot}P) - k_{-4}(M^*ADP{\cdot}P) - k_5(M^*ADP{\cdot}P) \quad (3)$$

$$d(M^*ADP)/dt = k_5(M^*ADP{\cdot}P) - k_{-5}(M^*ADP) - k_7'(M^*ADP) \quad (4)$$

$$d(M^*ATP)/dt = d(M^*ATP)/dt + k_7'(M^*ADP) \quad (5)$$

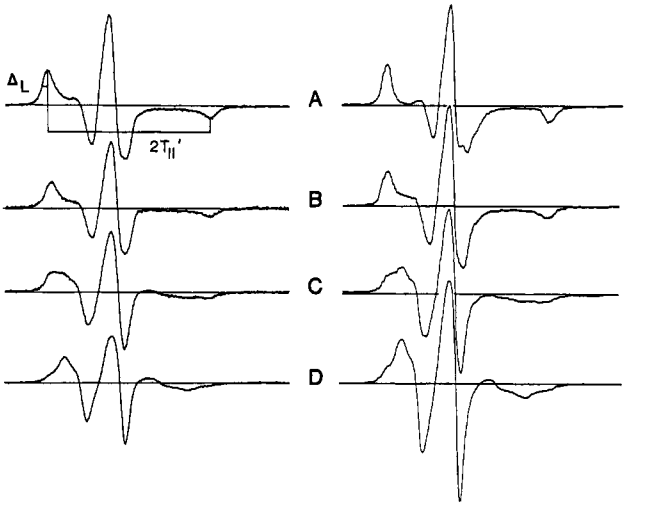

FIGURE 1: Conventional EPR spectra of IASL-labeled myosin filaments (left) and myosin monomers (right) in the presence and absence of nucleotides. (A) No nucleotide addition; (B) +5 mM MgADP; (C) +5 mM MgATP; (D) +5 mM MgADP and 5 mM VO_4^{3-}; 20 °C, base line 120 G.

The steps in Scheme II are numbered as in Bagshaw and Trentham (1974). Rate constants for unmodified myosin were taken from Webb and Trentham (1983) and Wells and Bagshaw (1984) and are as follows: $k_3 = 160\ s^{-1}$, $k_{-3} = 18\ s^{-1}$, $k_4 = 0.06\ s^{-1}$, $k_{-4} = 0.23\ M^{-1}\ s^{-1}$, and $k_5 = 10\ s^{-1}$. The value of k_{-5} is very small and was assumed to be 0.0, and k_7' which includes both the ADP dissociation and ATP association rate constants is very large and was set at $1000\ s^{-1}$. For the case of myosin modified at SH_1 with iodoacetic acid (IAA), Sleep et al. (1981) have shown that the most important perturbation of the reaction sequence occurs at the hydrolysis step, with k_3 falling to $25 \pm 5\ s^{-1}$ (16.7% of control). We have set k_3 to $25\ s^{-1}$ for the simulation of IASL-labeled myosin. The amplitude of the phosphate burst for IAA-S-1 as determined by Sleep et al. (1981) was 0.5–0.6 mol $site^{-1}$. Since the amplitude of the burst is $k_3/(k_3 + k_{-3})$, k_{-3} is 16.7–25 s^{-1}, so both of these extreme values for k_{-3} were tested in our simulations. For k_4, we used $0.60\ s^{-1}$ (10 times control), which we obtained by measuring the steady-state ATPase activity under EPR conditions. This compares favorably with $0.89\ s^{-1}$ measured by Sleep for IAA-labeled myosin (Sleep et al., 1981). Other rate constants were left unchanged. Alteration of the other rate constants in the scheme within the ranges suggested by the experiments of Sleep et al. (1981) did not significantly alter results of the simulations.

RESULTS

IASL-myosin. Figure 1 shows typical conventional (V_1) EPR spectra obtained for IASL-myosin monomers and filaments, and Table II shows the parameters derived from these and other spectra. At both high (μ = 0.50 M) and low (μ = 0.15 M) ionic strength in the absence of nucleotides, the EPR spectra are characteristic of strongly immobilized spin-labels (rotational correlation time $\tau_r > 10^{-7}$ s or order parameter $S > 0.9$). Since many of the previous studies were performed using myosin monomers (high ionic strength), we include spectra of monomers in Figure 1 for comparison. The remainder of this study focuses on myosin filaments (physiological ionic strength), but the observations are qualitatively similar for both conditions, and exceptions will be pointed out where they occur.

Nucleotide Additions. When ADP is added to IASL-myosin filaments (Figure 1, row B, left), there is a slight

Table II: Spectral Parameters[a]

sample	$2T_{\parallel}'$	Δ_L	N
IASL			
no Nuc	69.75 ± 0.39	2.36 ± 0.18	7
ADP	67.87 ± 0.42	2.58 ± 0.15	5
ATP	na	na	
ADP and V_i	na	na	
MSL			
no Nuc	68.30 ± 0.35	2.43 ± 0.14	3
ADP	68.16 ± 0.39	2.65 ± 0.19	5
ATP	68.00 ± 0.10	2.47 ± 0.02	2
ADP and V_i	66.19 ± 0.33	3.13 ± 0.24	6

[a] Spectral parameters of IASL and MSL myosin filaments. $2T_{\parallel}'$ represents the peak-to-peak splitting in gauss of the high- and low-field extrema. Δ_L represents the width in gauss of the outer portion of the low-field peak at half-height. N is the number of experiments combined for determination of the mean and standard error. The designation na indicates not applicable for those samples where more than one population of spins is evident and the interpretations of values for $2T_{\parallel}'$ and Δ_L are ambiguous. N is the number of determinations; the values are the mean ± SEM except for $N = 2$, where the uncertainty given is half the range. Buffers are given in Table I; temperature was 20 °C.

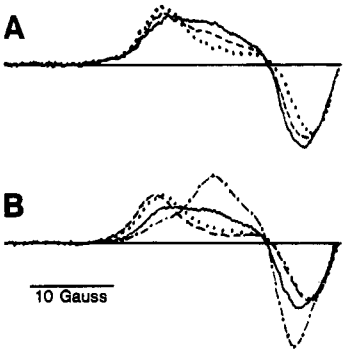

FIGURE 2: (A) Overlay of the EPR spectra of IASL-labeled myosin filaments as a function of time during ATPase activity (no ATP regenerating system employed). Solid line, acquisition of spectrum begun ~45 s after addition of ATP. Dashed line, acquisition of spectrum begun 3.6 min after addition of ATP. Dotted line, acquisition begun 8 min after addition of ATP. The time required to complete one scan (120 G) was 50 s. (B) Overlay of the EPR spectrum of myosin in the presence of ATP (solid line), ADP (dotted line), no nucleotide (dashed line), and ADP + vanadate (dots and dashes). 20 °C, base line 39.6 G.

narrowing of the spectrum, implying an increase in the probe's submicrosecond rotational mobility, in agreement with previous studies of IASL-myosin (Seidel et al., 1970; Seidel & Gergely, 1971). As shown in Table II, ADP induces a 1.9-G decrease in $2T_{\parallel}'$ and a 0.22-G increase in Δ_L. This would correspond to a decrease in the rotational correlation time from about 10 μs (Thomas et al., 1980) to about 80 ns, assuming isotropic motion (Marsh, 1981). Alternatively, assuming rapid restricted motions (Gaffney, 1976), the order parameter for subnanosecond motions has decreased from 1.0 to 0.96.

When ATP (Figure 1, row C) is added, new spectral features appear at magnetic field values nearer to the center of the spectrum than those of IASL-myosin ± ADP (Figure 1, rows A and B), confirming previous observations (Seidel & Gergely, 1971; Seidel, 1975; Wells & Bagshaw, 1984). These features must arise from more mobile probes, having both nanosecond (or subnanosecond) correlation times and large angular amplitudes (order parameters less than 0.6). Such probes are usually termed "weakly immobilized". The line shape in the presence of ATP indicates more probe mobility in monomers than in filaments.

Orthovanadate has been shown to inhibit the myosin ATPase by formation of a long-lived myosin–ADP–vanadate complex (Goodno, 1979). The long lifetime of this complex has raised the possibility that a stable myosin–product complex could be trapped and examined. A previous study has shown that vanadate and ADP induce a mobilization of the SH_1-bound iodoacetamide spin probe that is similar to that observed in the presence of ATP (Wells & Bagshaw, 1984). However, Figure 1 shows clearly that the spectra for the two additions are not identical: for both filaments and monomers, the spectrum in the presence of ADP and vanadate shows a greater shift of spectral intensity toward the center of the spectrum, indicating a greater degree of probe mobility than observed in the presence of ATP alone. The spectrum of IASL-labeled myosin + ADP and V_i was constant over a vanadate concentration range from 0.5 through 10 mM (data not shown). The lack of a dependence on V_i concentration supports the assumption that orthovanadate is the inhibiting vanadate species, since polymeric forms of vanadate dissociate in dilute solution (Chasten, 1983). ATP and vanadate added together (data not shown) produced a spectrum indistinguishable from that found when ADP and vanadate were added. The effect of AMPPNP on the spectrum of IASL-myosin was indistinguishable from that induced by the addition ADP (data not shown). Addition of ATPγS (an ATP analogue slowly hydrolyzed by myosin) to IASL-myosin filaments results in a spectrum that is similar in line shape to that induced by addition of either ADP or AMPPNP (data not shown).

Isoclinic Points. An isoclinic point, defined as a common point of intersection in a set of derivative absorption spectra (e.g., conventional EPR spectra), has essentially the same interpretation as an isosbestic point for a set of absorption spectra: it strongly suggests the presence of a linear combination of two interconverting species that are spectrally distinguishable (Marriott & Griffith, 1974).

In Figure 2A, the low-field region of the V_i spectrum of IASL-myosin is shown as a function of time after ATP addition. As the ATP is depleted, the shape of the spectrum shifts from a broad multicomponent spectrum to a spectrum indistinguishable from the single-component spectrum obtained in the presence of ADP (Figure 1, row B, left). For this overlay, a clear isoclinic point is evident, suggesting that the ATP line shape may be composed of an internally linear set of conformations of which the ADP line shape is one of two spectrally distinguishable components. Figure 2B shows the overlay of the spectra of IASL-myosin in the absence of nucleotides and in the presence of ATP, ADP, and ADP + V_i. This overlay contains an isoclinic point at the same magnetic field position as that seen in the ATP depletion experiment of Figure 2A and suggests that both the broad ADP spectrum and the narrow ADP + V_i spectrum are components of the ATP spectrum. In fact, the shoulder at the low-field end of the ADP + V_i spectrum suggests that it, too, contains a significant contribution from the ADP spectrum, i.e., that the ATP and ADP + V_i spectra are both composites of two components, one of which has the same line shape as the ADP spectrum. In contrast, the overlay of the spectrum of myosin in the absence of nucleotides on the spectra in the presence of nucleotides (Figure 2B) makes it apparent that, while the no-nucleotide line shape is similar to that of IASL-myosin + ADP, it is not a component in the spectra observed in the presence of nucleotides.

Spectral Subtractions. Since isoclinic points suggest that spectra in the presence of ATP and ADP + vanadate contain contributions from two principal conformational states, we used computer subtractions to resolve the spectra into their intrinsic components. The spectrum in Figure 3C was obtained by

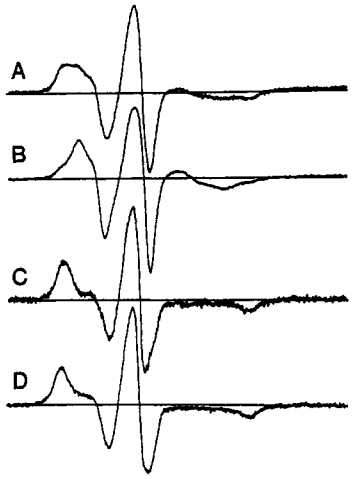

FIGURE 3: Subtraction of IASL-myosin + ADP and V_i spectrum from that of IASL-myosin + ATP. (A) Spectrum of myosin in the presence of ATP, during steady-state ATPase activity. (B) Spectrum of myosin in the presence of ADP and V_i. (C) Difference spectrum generated by digital subtraction of 44% of spectrum B from spectrum A. (D) Spectrum of IASL-myosin in the presence of ADP alone. 20 °C, base line 120 G.

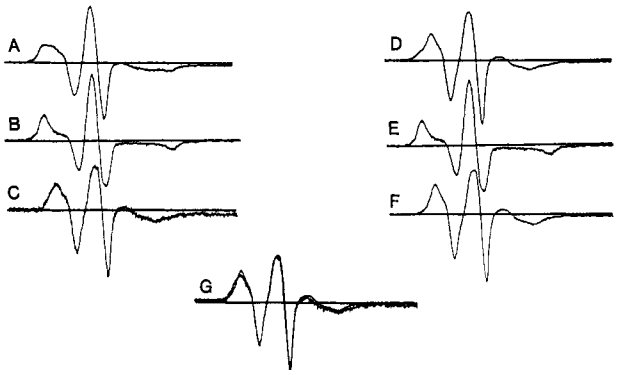

FIGURE 4: Comparison of the ATP − ADP and (ADP + V_i) − ADP difference spectra. (A) Conventional EPR spectrum of myosin + ATP. (B) Spectrum of myosin–ADP. (C) Difference spectrum produced by the subtraction of 48% of spectrum B from spectrum A. (D) Conventional EPR spectrum of myosin plus ADP + V_i. (E) Spectrum of myosin–ADP. (F) Difference spectrum produced by the subtraction of 22% of spectrum E from spectrum D. (G) Overlay of difference spectra C and F. 20 °C, base line 120 G.

subtracting the ADP + V_i spectrum from the ATP spectrum until the sharp features corresponding to mobile probes were removed from the ATP spectrum. This difference spectrum was an unambiguous end point, and the resulting line shape is virtually indistinguishable from the ADP spectrum (Figure 3D). Equivalently, the ATP spectrum (Figure 3A) can be simulated by adding the ADP and ADP + V_i spectra (data not shown). These results further confirm that, of the two spectrally distinguishable components in the IASL-myosin + ATP spectrum, one is indistinguishable from that sensed by the probe for myosin + ADP.

Using the line shape of myosin + ADP as a model for one of the motional components in myosin + ATP, we then used computer subtraction to quantitate the "mobile" and "immobile" components contained in the ATP spectrum (Figure 4, left). For the remainder of this discussion, the immobile fraction of spins will refer to the fraction of the ADP spectrum that was subtracted to remove the intensity from the spectral wings. For the ATP spectrum, this fraction was 0.48. As shown in Figure 4C, the residual 52% of the spectral intensity is a sharp-featured spectrum whose line shape implies rapid ($\tau_r < 10$ ns) large-amplitude ($S < 0.6$) rotational motion.

Table III: Relative Populations of the Two Nucleotide-Induced Motional Components[a]

sample	% mobile	mobile/immobile	N
myosin filaments			
ADP	0	0	
ATP	51.6 ± 0.4	1.07 ± 0.02	4
ADP + V_i	80.2 ± 0.1	4.05 ± 0.03	4
myosin monomers			
ADP	0	0	
ATP	48.9 ± 6.0	0.98 ± 0.25	8
ADP + V_i	60.2 ± 3.3	1.53 ± 0.23	6

[a] The relative populations of the two nucleotide-induced motional components as determined by spectral subtraction. The immobile component represents the fraction of spins giving rise to a line shape that can be approximated by the line shape of IASL-myosin–ADP. The mobile component represents the residual spin population whose rotational motion exceeds that of the spins in the immobile component by approximately an order of magnitude. The values are the mean ± standard error of the mean (SEM); N is the number of determinations. Buffers are given in Table I; temperature was 20 °C.

Spectral parameters obtained from this difference spectrum (Figure 4C) indicate that the rotational correlation time of the mobile component has decreased to about 9 ns, assuming isotropic rotational motion (Marsh, 1981), as compared to 10 μs in the absence of nucleotides (Thomas et al., 1980) and 80 ns in the presence of MgADP (discussed above). Alternatively, assuming rapid restricted motion (Gaffney, 1976), the order parameter for subnanosecond motion has decreased to 0.54, as compared with 1.0 in the absence of nucleotides and 0.96 in the presence of MgADP (discussed above).

To test the hypothesis that the ADP spectrum is also a component of the ADP + V_i spectrum, an analogous subtraction was performed (Figure 4, right). After subtraction of 20% of the ADP spectrum from the ADP + V_i spectrum, the intensity in the wings was removed. At the bottom of Figure 4, the difference spectra obtained by removing the ADP-like component from the ATP and ADP + V_i spectra are overlayed. The match between the two difference spectra indicates that the mobile spin populations for the two samples are sensing similar local conformations. The major difference between the two samples is, therefore, the ratio of the fraction of probes which sense the ADP-like (immobile) conformation to the fraction that sense the more mobile conformation.

The results of the subtractions of the ADP line shape from the ATP and ADP + V_i spectra for myosin filaments and myosin monomers are shown in Table III. The results are similar for filaments and monomers, but V_i has a smaller effect on the percentage of mobile probes in monomers than in filaments.

As mentioned previously, the ATP-induced line shape can be reconstructed by the addition of the spectra of IASL-myosin + ADP and IASL-myosin + ADP and V_i. As an alternative means of determining the relative concentrations of the populations present, we simulated the ATP spectrum as a linear combination of the mobile component (Figure 4F) and that of myosin + ADP (Figure 4E). The fractions of the two components were varied to minimize the residual between the sum and Figure 4A. The fit was excellent (not shown), and the fractions of the two components in the presence of ATP agreed with those in Table III.

Variation of the temperature in the presence of ADP + vanadate resulted in changes in the relative populations of the two fractions. When the temperature was reduced, the ADP-like fraction increased. At no temperature in the range of 0–37 °C could a single-component spectrum be induced, and the return to 20 °C always occurred without hysteresis

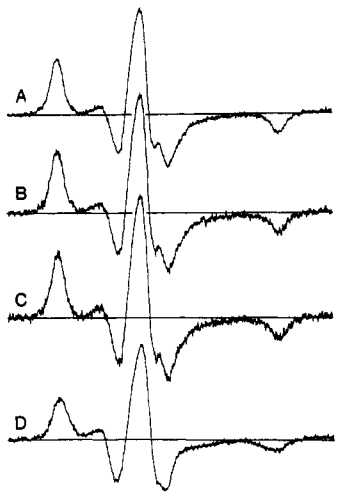

FIGURE 5: EPR spectra of MSL-myosin filaments in the presence and absence of nucleotides. (A) No addition; (B) +5 mM MgADP; (C) +5 mM MgATP; (D) +5 mM ADP and 5 mM VO_4^{3-}. Note that only the spectrum of myosin in the presence of ADP and vanadate shows any nucleotide-dependent effects (see Table II); 20 °C, base line 100 G.

(data not shown). Similarly, in the presence of ADP, probe mobility decreased (as determined by changes in $2T_{\parallel}'$ and Δ_L) as the temperature decreased. At no temperature (range 0–40 °C) did the mobility of the ADP line shape approach that of the mobile component observed in the presence of ATP or ADP + vanadate (data not shown).

MSL-myosin. It has been demonstrated previously that MSL bound to SH_1 is relatively insensitive to nucleotides binding to the active site of myosin (Thomas et al., 1980). This is confirmed by the spectra in Figure 5 (A–C). These spectra, whose parameters are in Table II, show that the conformational changes detected by IASL in the presence of ADP and ATP are not detected by MSL. No significant changes in either $2T_{\parallel}'$ or Δ_L were induced by either ADP or ATP, implying no probe motion independent of the motion of the myosin head. Similarly, the lack of changes in ST-EPR spectra of MSL-myosin (not shown) show that the overall mobility of myosin heads is also not affected by ADP or ATP [as shown previously by Thomas et al. (1980)]. The differences in the sensitivity of IASL and MSL are intriguing, since ATPase activities and labeling competition studies suggest strongly that the signals observed in both cases arise from probes bound to SH_1. Such differential responses to nucleotides have also been observed for fluorescent probes at SH_1 [reviewed by Cooke (1986) and Thomas (1987)]. In particular, some fluorescent probes at SH_1 undergo large movements in response to ADP, while others do not (Borejdo et al., 1982).

The addition of ADP and vanadate to MSL-myosin filaments induces a significant mobilization of the probe (Figure 5D; Table II), as previously reported by Wells & Bagshaw (1984). However, no spectral change is observed during steady-state ATP hydrolysis (Figure 5C). Thus, both MSL and IASL show that the conformation of myosin with ADP and vanadate bound is different from the conformation of myosin during steady-state ATP hydrolysis. However, the spectrum of MSL-myosin + ATP is not a linear combination of the spectra of MSL-myosin + ADP and MSL-myosin + ADP and V_i, in contrast to the results obtained for IASL-labeled myosin. There are two alternative interpretations: (1) This provides further evidence that IASL has a different sensitivity to myosin's conformational changes than has MSL. MSL can detect that the predominant conformation of myosin + ADP and V_i is distinct from both predominant conformations of myosin during steady-state ATP hydrolysis, while IASL cannot. (2) The effect of labeling on myosin's conformational state is different for MSL than it is for IASL.

Discussion

Summary of Spectral Interpretation. We have examined quantitatively the changes in the local conformation about the SH_1 residue of the myosin head when nucleotides bind to the active site under physiological conditions. Through the use of conventional EPR and selective spin-labeling, we have resolved the predominant conformations present during steady-state ATP hydrolysis and compared these with those induced by ADP, ±vanadate, and ATP analogues. In the absence of nucleotides, both IASL (Figure 1A) and MSL (Figure 5A) probes have EPR spectra characteristic of strongly immobilized probes (no submicrosecond motions), confirming previous studies showing that both probes report the overall motion of the heads (Seidel et al., 1970; Thomas, 1975; Thomas et al., 1980). ADP induces a slight but significant nanosecond mobilization of IASL, while ATP induces a much greater nanosecond mobilization (Figure 1, Table II). In contrast, MSL is unaffected in both the nanosecond range (Figure 5, Table II) and the microsecond range (Thomas et al., 1980). Thus, ADP and ATP affect the internal conformation of the myosin head without greatly changing its shape. In the presence of ATP, the IASL spectra are consistent with the presence of two previously unresolved conformations (by steady-state methods), one indistinguishable from that induced by ADP and the other similar to the predominant component induced by vanadate in the presence of either ADP or ATP. These conclusions are supported by the isoclinic points in Figure 2 and the spectral subtractions in Figures 3 and 4, which suggest further that two conformations similar to those induced by ATP are induced in the presence of ADP + vanadate. The ratio of the ADP-like population to the more mobile population is 1:1.1 during steady-state ATP hydrolysis and is 1:4 in the presence of ADP + vanadate.

Assignment of EPR-Detected Conformations to Intermediates in the ATPase Cycle. Using literature values for the rate constants of the intermediate steps in the hydrolysis of ATP by myosin, our simulation routine correctly reports that the predominant states in Scheme II during ATP hydrolysis by unmodified myosin in the steady state are the M*ATP and M**ADP·P_i states in a ratio of 1:9 (Bagshaw & Trentham, 1974). By employing the rate constants for myosin modified at SH_1 (see Materials and Methods), we arrive at the same two predominant states for SH_1-modified myosin, with a change in their relative proportions. Our program predicts that 97–99% of the myosin during steady-state ATP hydrolysis will still be in the M*ATP and M**ADP·P_i states, with the ratio of the states in the range of 1:1.4 to 1:1. This result is supported by the report that the amplitude of the phosphate burst for IAA-S-1 is 0.50 mol $site^{-1}$ (Sleep et al., 1981), indicating that the ratio of the two states is about 1:1. Bagshaw and Warriner (personal communication) have followed the time course of the fluorescence change during MgATP turnover at 20 °C for unmodified S-1 and IASL-S-1. Upon spin-labeling, the fluorescence enhancement of the steady-state intermediates is about half of that of unlabeled S-1, as would be expected if the phosphate burst is about 0.5 for IASL-S-1.

Since the chemical kinetics simulations yield the same ratio (about 1:1) for the two predominant chemical states (M*ATP and M**ADP·P_i) as found for the two predominant EPR motional states (immobile and mobile), we propose that these pairs of chemical and conformational states are identical. The remaining problem is to determine which of the two chemical

states to assign to the immobile spectral component. The spectra of myosin plus either of the nonhydrolyzable ATP analogues AMPPNP and ATPγS are similar to the immobile ADP-like component, strongly suggesting that the conformation of the myosin–ATP complex before hydrolysis (M*ATP) corresponds to the immobile (ADP-like) probe population. Vanadate forms a complex with ADP and myosin (M^{t}·ADP·V_i) that is similar to the M**ADP·P_i state (Goodno, 1979, 1982; Wells & Bagshaw, 1984). Since the mobile population is predominant in the presence of ADP and V_i, we assign the mobile conformation to the M**ADP·P_i state. These assignments support a model in which the spectra acquired during steady-state ATP hydrolysis report the relative concentrations of two interconverting "weak-binding" states of myosin (Greene & Eisenberg, 1980). While this interpretation is somewhat dependent on the rate constants of Sleep et al. (1981), the results of Bagshaw and Warriner (personal communication) confirm that the effects of IAA and IASL on the myosin ATPase are comparable.

A possible criticism of these assignments is that when ATP becomes depleted, the buildup of ADP would result in the generation of a spectral component whose line shape could not be resolved from that of the proposed M*ATP conformation. However, the ATP concentration used (5 mM) and the ATP regenerating system (20 mM creatine phosphate and 233 IU of creatine phosphokinase) provided for the acquisition of several identical scans during the time period that ATP would still be saturating (~8 min). Increasing the initial ATP concentration to 10 or 15 mM (compensating for ionic strength with potassium acetate) did not change the steady-state spectrum, and the kinetic simulations returned a [myosin-ADP]/[total myosin] of <1%. In addition, Bagshaw and Warriner (personal communication) have observed the stopped-flow fluorescence of IASL-S-1 + ATP and noted that the shape of the curve as the fluorescence increases shows no overshoot of the final steady-state fluorescence intensity, indicating the lack of a significant contribution of the M*ADP state as a steady-state intermedate (Bagshaw, 1975).

An assumption inherent in the assignments proposed in this study is that the conformational states detected by EPR have a 1:1 correlation with the chemical states of the nucleotide in the active site of myosin. The possibility remains that a single chemical state of a nucleotide could give rise to more than one conformation of myosin and that a change in the chemical state simply changes the equilibrium between the states present (Shriver, 1984). However, the agreement between the kinetic simulations and quantitation of spin states in the present study has allowed us to make assignments while employing the assumption of a 1:1 correlation of chemical and conformational states, without invoking the presence of other conformational pathways. A transition between different conformational states with the same chemical identity has been proposed for myosin + ADP and V_i (Scheme III; Goodno, 1979, 1982). Although the spectrum of M + ADP and V_i is nearly identical with that of the mobile conformation, which we have assigned to M**ADP·P_i, the presence of a small but significant second (ADP-like) spectral component suggests that M^{t}·ADP·V_i is conformationally heterogeneous. If, as previously proposed, M^{t}·ADP·V_1 corresponds closely to M**ADP·P_i, this suggests that M**ADP·P_i could also be a conformationally heterogeneous chemical state. However, the ADP-like component makes a very small contribution to the M^{t}·ADP·V_i spectrum, and it is plausible that a small amount of *chemical* heterogeneity is present in this sample that is not present in M**ADP·P_i. The assignment of a chemical state to the immobile population in the presence of ADP and vanadate is as yet unresolved. It is likely that the two conformations observed in the spectrum of IASL-myosin + ADP and V_i represent the equilibrium between two previously proposed M·ADP·V_i complexes (Scheme III; Goodno, 1979). An extension of this line of speculation is that the M*ADP·P_i conformation of myosin, if isolated, would yield a spectrum resembling that of the immobile or "ADP-like" spectral component in these studies.

Scheme III

$$M + ADP + V_i \rightarrow M{\cdot}ADP{\cdot}V_i \leftrightarrow M^{t}{\cdot}ADP{\cdot}V_i$$

Relationship to Other Work. The nucleotide-dependent changes we have observed in the V_1 spectra of IASL-labeled myosin are in qualitative agreement with previous results by other investigators (Seidel et al., 1970; Stone, 1970; Seidel & Gergely, 1971, 1973; Blumenfeld & Ignateva, 1974; Wells & Bagshaw, 1984; Yamada et al., 1984; Furukawa & Tonomura, 1982). In comparing the assignments of states to the probe populations in our EPR spectra, we find general agreement with the original assignments of Seidel and Gergely (1971). However, their assignments referred only to the predominant conformation present, while we have resolved the conformations, more precisely determined their chemical composition, and determined their relative concentrations during steady-state ATP hydrolysis. Previous studies had their quantitative interpretations limited by experimental factors that have been improved upon in the present study. In most of these studies, weakly immobilized probes were often visible in the absence of nucleotides, suggesting that the specificity of labeling of SH_1 was less than in the present study. Specific labeling of one site is required for the resolution of multiple states and the determination of their respective fractions. None of the previous studies utilized computer-assisted spectral subtraction, which are required to deconvolute multicomponent spectra and demonstrate convincingly the presence of the multiple spin species that are indicative of multiple conformations.

Nucleotide-induced changes in the intrinsic fluorescence of myosin have been cited as evidence for multiple conformational changes within myosin (see Scheme I). Consistent with the results of the present study, intrinsic fluorescence detects a greater change in myosin conformation during steady-state ATP hydrolysis than when ADP alone is bound or when ATP is bound before hydrolysis (Werber, 1972; Bagshaw, 1974), and continuous-wave fluorescence measurements during chemical transients have been used to resolve these changes in time during the ATPase cycle (Bagshaw, 1974, 1975; Bêchet et al., 1979; Trybus & Taylor, 1982). However, the resolution of the continuous-wave fluorescence technique is not sufficient to distinguish the simultaneous presence of distinct conformations of the enzyme in the steady state of ATP hydrolysis. Time-resolved fluorescence measurements using pulsed excitation could, in principle, resolve these components if they correspond to distinct lifetimes or correlation times.

NMR studies have also provided evidence suggesting multiple conformations of myosin. The ^{31}P NMR spectrum of ADP bound to S-1 shows two resolved β-phosphate peaks at 5 °C but only one at 25 °C, suggesting a temperature-dependent equilibrium between two different conformations of the active site (Shriver & Sykes, 1981a,b). A ^{19}F NMR probe attached to SH_1 on S-1 by an iodoacetamide linkage has a nucleotide-, temperature-, and pH-dependent chemical shift that appears to have two limiting values, although there were no resolved multiple resonances that could provide clear evidence for distinct protein conformations (Shriver & Sykes,

1982). In contrast to the behavior of the ^{31}P NMR, but consistent with the present results for IASL-SH_1, there was very little temperature dependence of the ^{19}F SH_1 probe in the presence of ADP or AMPPNP, and there was no difference between the effects of ADP and AMPPNP, suggesting that the limiting "states" observed by ^{19}F NMR at SH_1 do not correspond to those observed by ^{31}P NMR at the active site. The present EPR study differs from these NMR studies in several important ways: (a) we observed very little temperature dependence in the absence of nucleotides; (b) the two predominant states in the presence of nucleotides are conformationally distinct from that observed in the absence of nucleotides; (c) intact myosin was studied; (d) experiments were performed in the presence of ATP (i.e., during the steady state of ATP hydrolysis) and ADP + V_i; and (e) resolved EPR signals (observed under the latter conditions) provide direct evidence for two interconverting conformational states of myosin at a site removed from the active site.

Since specific labeling of SH_1 has been achieved in myofibrils (Thomas et al., 1980) and in glycerinated muscle fibers (Barnett et al., 1984), further EPR studies should aid in the resolution of myosin's conformational states in intact muscle.

ACKNOWLEDGMENTS

We thank Dr. Piotr Fajer for helpful discussions, Dr. Piotr Fajer and R. L. H. Bennett for assistance with computer programming, Sandra Johnson for assistance with biochemical preparations, Dr. John Lipscomb for making the Varian E-109 spectrometer and computer available, and Dr. Clive Bagshaw for his critical reading of the manuscript, his insightful comments, and his communication of unpublished results.

Registry No. IASL, 25713-24-0; ADP, 58-64-0; ATPase, 9000-83-3; MgATP, 1476-84-2; MgADP, 7384-99-8; VO_4^{3-}, 14333-18-7.

REFERENCES

Bagshaw, C. R. (1975) *FEBS Lett. 58*, 197–201.
Bagshaw, C. R., & Trentham, D. R. (1974) *Biochem. J. 141*, 331–379.
Bagshaw, C. R., & Reed, G. H. (1976) *J. Biol. Chem. 251*, 1975–1983.
Barnett, V. A., & Thomas, D. D. (1984) *J. Mol. Biol. 179*, 83–102.
Barnett, V. A., Svensson, E. C., & Thomas, D. D. (1984) *Biophys. J. 45*, 100a.
Bechet, J.-J., Breda, C., Guinand, S., Hill, M., & d'Albis, A. (1979) *Biochemistry 18*, 4080–4089.
Blumenfeld, L. A., & Ignateva, L. G. (1974) *Eur. J. Biochem. 47*, 75–79.
Borejdo, J., Assulin, O., Ando, T., & Putnam, S. (1982) *J. Mol. Biol. 158*, 391–414.
Chasten, N. D. (1983) *Struct. Bonding (Berlin) 53*, 105–138.
Cheung, H. (1969) *Biochim. Biophys. Acta 194*, 478–485.
Cooke, R. (1986) *CRC Crit. Rev. Biochem. 21*, 53–118.
Crowder, M. S., & Cooke, R. (1984) *J. Muscle Res. Cell Motil. 5*, 131–146.
Eads, T. M., Austin, R. H., & Thomas, D. D. (1984) *J. Mol. Biol. 179*, 55–81.
Furukawa, K.-I., & Tonomura, Y. (1982) *J. Biochem. (Tokyo) 92*, 1219–1225.
Gaffney, B. J. (1976) in *Spin Labeling* (Berliner, L. J., Ed.) Appendix IV, pp 567–571, Academic Press, New York.
Geeves, M. A., & Trentham, D. R. (1982) *Biochemistry 21*, 2207–2214.
Gellert, M. F., & Englander, S. W. (1963) *Biochemistry 2*, 39–42.
Goodno, C. C. (1979) *Proc. Natl. Acad. Sci. U.S.A. 76*, 2620–2624.
Goodno, C. C. (1982) *Methods Enzymol. 85 (B)*, 116–123.
Graceffa, P., & Seidel, J. C. (1980) *Biochemistry 19*, 33–39.
Greene, L., & Eisenberg, E. (1980) *Proc. Natl. Acad. Sci. U.S.A. 77*, 2616–2620.
Highsmith, S., & Cooke, R. (1983) *Cell Muscle Motil. 4*, 207–236.
Highsmith, S., Kazuyuki, A., Konrad, M., Goody, R., Holmes, K., Wade-Jardetsky, N., & Jardetsky, O. (1979) *Biochemistry 18*, 4238–4244.
Huxley, H. E. (1969) *Science (Washington, D.C.) 164*, 1356–1366.
Huxley, A. F., & Simmons, R. (1971) *Nature (London) 233*, 533–538.
Lipscomb, J. D., & Salo, R. W. (1983) *Comput. Enhanced Spectrosc. 1*, 11–15.
Marriott, T. B., & Griffith, O. H. (1974) *J. Magn. Reson. 13*, 45–52.
Marsh, D. (1981) in *Membrane Spectroscopy* (Grell, E., Ed.) pp 51–142, Springer-Verlag, New York.
Mason, R. P., & Freed, J. H. (1974) *J. Phys. Chem. 78*, 1321–1323.
Morales, M. F., Borejdo, J., Botts, J., Cooke, R., Mendelson, R. A., & Takashi, R. (1982) *Annu. Rev. Phys. Chem. 33*, 319–351.
Morita, F. (1967) *J. Biol. Chem. 242*, 4501–4506.
Morita, F. (1977) *J. Biochem. (Tokyo) 81*, 313–320.
Pribil, R. (1972) *Analytical Applications of EDTA and Related Compounds*, pp 304–305, Pergamon Press, Oxford.
Reiger, P. H. (1973) *Aust. J. Chem. 26*, 1173–1181.
Seidel, J. C. (1975) *J. Biol. Chem. 250*, 5681–5687.
Seidel, J. C., & Gergely, J. (1971) *Biochem. Biophys. Res. Commun. 44*, 826–830.
Seidel, J. C., & Gergely, J. (1973) *Arch. Biochem. Biophys. 158*, 853–863.
Seidel, J. C., Chopek, M., & Gergely, J. (1970) *Biochemistry 9*, 3265–3272.
Sekine, T., & Kielley, W. W. (1964) *J. Biochem. (Tokyo) 54*, 196–198.
Shriver, J. W. (1984) *Trends Biochem. Sci. (Pers. Ed.) 9*, 322–328.
Shriver, J. W., & Sykes, B. D. (1981a) *Biochemistry 20*, 2004–2012.
Shriver, J. W., & Sykes, B. D. (1981b) *Biochemistry 20*, 6357–6362.
Shriver, J. W., & Sykes, B. D. (1982) *Biochemistry 21*, 3022–3028.
Sleep, J. A., Trybus, K. M., Johnson, K. A., & Taylor, E. W. (1981) *J. Muscle Res. Cell Motil. 2*, 373–399.
Squier, T. C., & Thomas, D. D. (1986) *Biophys. J. 49*, 921–935.
Stone, D. (1970) *Arch. Biochem. Biophys. 141*, 378–380.
Thomas, D. D. (1987) *Annu. Rev. Physiol.* (in press).
Thomas, D. D., & Cooke, R. (1980) *Biophys. J. 32*, 891–906.
Thomas, D. D., Seidel, J. C., Gergely, J., & Hyde, J. S. (1975) *J. Supramol. Struct. 3*, 376–390.
Thomas, D. D., Ishiwata, S., Seidel, J. C., & Gergely, J. (1980) *Biophys. J. 32*, 873–890.
Tonomura, Y., Appel, P., & Morales, M. F. (1966) *Biochemistry 5*, 515–521.
Trentham, D. R., Eccleston, J. F., & Bagshaw, C. R. (1976) *Q. Rev. Biophys. 9*, 217–281.
Trybus, K. M., & Taylor, E. W. (1979) *Biophys. J. 25*, 21a.

Webb, M. R., & Trentham, D. R. (1983) in *Handbook of Physiology, Section 10: Skeletal Muscle* (Peachy, L. D., Adrian, R. H., & Geiger, S. R., Eds.) Chapter 8, pp 237–255, Williams & Wilkins, Baltimore, MD.

Wells, C., & Bagshaw, C. R. (1984) *J. Muscle Res. Cell Motil. 5*, 97–112.

Werber, M., Szent-Györgyi, A. G., & Fasman, G. (1972) *Biochemistry 11*, 2872–2882.

Wiberg, K. B. (1974) in *Techniques in Chemistry*, 3rd ed., Vol. IV, Chapter 13, pp 741–776, McGraw-Hill, New York.

Yamada, T., Kirino, Y., & Shimizu, H. (1984) *J. Biochem. (Tokyo) 96*, 1021–1026.